Supporting Information

New Heteroleptic Iridium Complexes Having One Biphenyl-2,2'-diyl and Two Bipyridyl Based Ligands

Kyu Reon Lee†, Min-Sik Eum†, Chong Shik Chin†, Seung Chan Lee‡, In June Kim‡,
Young Sik Kim‡, Youngmee Kim§, Sung-Jin Kim§, Nam Hwi Hur†*

†Department of Chemistry, Sogang University, Seoul 121-742, Korea,
‡Department of Science and Department of Information Display Engineering,
Hongik University, Seoul 121-791, Korea,
§Department of Chemistry and Nano Science, Ewha Womans University, Seoul 120-750,
Korea.

General. ^{1}H-NMR and ^{13}C-NMR spectra were obtained using a Varian Gemini-300 (300 MHz for ^{1}H) and Varian Inova-500 (500 MHz for ^{1}H, and 125 MHz for ^{13}C) spectrometer. Elemental analyses were performed using a Carlo Erba EA 1180 elemental analyzer in the Organic Chemistry Research Center at Sogang University. High resolution mass spectra were recorded on a 4.7 Tesla Ion Spec ESI-FTMS and a Micromass LCT ESI-TOF mass spectrometer.

X-ray Crystallography. The X-ray diffraction data were collected on a Bruker SMART APEX diffractometer equipped with a monochromater using a Mo Kα (λ = 0.71073 Å) incident beam. A crystal was mounted on a glass fiber. The CCD data were integrated and scaled using the Bruker-SAINT software package. The structure was solved and refined using SHEXTL V6.12 (SHELXTL/PC Version 6.12 for Windows XP 2001, Bruker AXS Inc., Madison, Wisconsin, USA). All hydrogen atoms were placed in the calculated positions. All bond lengths in a OTf$^-$ anion were fixed and refined isotropically. Single crystals of **2** were grown by slow transfer of diethylether vapor into 10^{-3} M of acetonitrile solution of **2** at 4℃. The crystallographic data for **2** are listed in Table S1, and the selected bond lengths and angles are listed in Table S2.

Theoretical Calculations. Calculations of the electronic ground states for **1** and **2** were carried out using the B3LYP density functional theory (DFT). LANL2DZ[3] and 6-31G (d)[2] basis sets were employed for iridium and the other atoms, respectively. For the calculated ground state geometries, the electronic structure was examined in terms of the highest occupied molecular orbitals (HOMOs) and the lowest unoccupied molecular orbitals (LUMOs). The electronic populations on the central atom were calculated to show the significant admixture of ligand π character with the amount of iridium 5*d* character in the occupied molecular orbitals, related to the metal-to-ligand charge-transfer (MLCT) transitions.

Photochemistry. Due to the quenching of the phosphorescence by aerobic oxygen, all the measurements were made at room temperature under the argon atmosphere. Absorption spectra were measured on an Agilent 8453 UV-visible spectrophotometer. Emission spectra were measured on a HITACHI F-7000 spectrometer, using excitation wavelengths of 325 nm for **1** and **2**. Quantum efficiency was calculated with reference to a $[Ru(bpy)_3]Cl_2$ standard value (Φ_{pl}= 0.028).

Synthesis of [Ir(cod)(biph)Cl]$_2$. The compound was synthesized by the method reported by Crabtree et al., in which [Ir(cod)Cl]$_2$ dimer in dichloromethane was treated with biphenylene under N_2 and heated for 2 h at 90 ^{o}C in a screw-cap vial.[3]

Synthesis of [Ir(cod)(biph)(bpy)](OTf). [Ir(cod)(biph)Cl]$_2$ (518 mg, 0.5 mmol), silver trifluoromethylsulfonate (AgOTf) (282.6 mg, 1.1 mmol), and 2,2'-dipyridyl (156.18 mg, 1 mmol) were placed in a 100 mL of round-bottom flask. A 25 mL of dichloromethane was added into the flask. The resulting solution was stirred for 1 h, which was then filtered through Celite. The filtrate was evaporated to a volume of 1 mL. To this solution a 300 mL of n-pentane was slowly added with vigorous stirring. The yellow precipitates were immediately formed, which were collected by filtration and washed with n-pentane and diethylether. The yellow product was dried under vacuum. The yield is 75 %. ^{1}H NMR (300 MHz; CD_3CN): δ 9.482 (d, J = 9.5 Hz, 1H), δ 8.379 (d, J = 13 Hz, 1H), δ 8.301 (t, J = 12.5 Hz, 1H), δ 8.212-8.517 (m, 2H), δ 8.038-8.018 (m, 2H), δ 7.809 (t, J = 12.5 Hz, 1H), δ 7.494 (t, J = 8.5 Hz, 1H), δ 7.328 (d, J = 12 Hz, 1H), δ 7.261-7.236 (m, 2H), δ 7.161 (t, J = 11 Hz, 1H), δ 6.677 (t, J = 11.5 Hz, 1H), δ 6.456 (t, J = 11.5 Hz, 1H), δ 5.913 (d, J = 13z, 1H), δ 5.377 (q, J = 13 Hz, 1H), δ 4.330-4.234 (m, 2H), δ 3.473 (t, J = 11 Hz, 1H), δ 2.927-2.793 (m, 2H), δ 2.710-2.600 (m, 1H), δ 2.494-2.382 (m, 2H), δ 2.149-2.039 (m, 1H), δ 1.802-1.786 (m, 2H).

Synthesis of [Ir[biph)(bpy)$_2$](OTf) (1). [Ir(cod)(biph)(bpy)](OTf) (394 mg, 0.5 mmol) and 2,2'-dipyridyl (85.91 mg, 0.55 mmol) were placed in a 100 mL of round-bottom flask. A 20 mL of 2-ethoxyethanol was added, which was then refluxed for 10 h under N_2. After cooling the solution down to room temperature, a 300 mL of diethylether was added with vigorous stirring. The reddish precipitates were formed, which were collected by filtration and washing with n-pentane and diethylether. The crude product was purified by chromatographic grade activated alumina using acetonitrile. The yield is 78 %. ^{1}H NMR (500 MHz; CD_3CN): δ 8.499 (d, J = 8 Hz, 2H), δ 8.417 (d, J = 8 Hz, 2H), δ 8.217 (d, J = 5.5 Hz, 2H), δ 8.165 (t, J = 8 Hz, 2H), δ 7.999 (t, J = 8 Hz, 2H). δ 7.857 (d, J = 5.5 Hz, 2H), δ 7.537 (d, J = 5.5 Hz, 2H), δ 7.519 (d, J = 4 Hz, 2H), δ 7.317 (d, J = 6.75 Hz, 2H), δ 6.900 (t, J = 7.5 Hz, 2H), δ 6.642 (t, J = 7.5 Hz, 2H), δ 6.101 (d, J = 7.5 Hz, 2H). ^{13}C NMR (125 MHz, CD_3CN): δ 158.456, 156.167, 154.721, 153.534, 149.631, 149.455, 140.074, 139.209, 132.545, 129.330, 128.978, 127.320, 125.642, 125.273, 124.668, 121.647. Elemental Analysis: Found: C, 49.0254; H, 2.9648; N, 7.0458 %. Calc. for $IrC_{33}H_{24}N_4O_3F_3S$: C, 49.18; H, 3.00; N, 6.95 %. HRMS: m/z found 657.2224, calculated for $IrC_{32}H_{24}N_4$ 657.16.

Synthesis of [Ir(cod)(biph)(dmbpy)](OTf). $[Ir(cod)(biph)Cl]_2$ (518 mg, 0.5 mmol), silver trifluoromethylsulfonate (AgOTf) (282.6 mg, 1.1 mmol), and 4,4'-dimethyl-2,2'-dipyridyl (202.6 mg, 1.1 mmol) were placed in a 100 mL of round-bottom flask. A 25 mL of dichloromethane was added into the flask. The resulting solution was stirred for 1 h, which was then filtered through Celite. The filtrate was evaporated to a volume of 1 mL. To this solution a 300 mL of n-pentane was slowly added with vigorous stirring. The yellow precipitates were immediately formed, which were collected by filtration and washed with n-pentane and diethylether. The yellow product was dried under vacuum, whose yield is 74%. ^{1}H NMR(300 MHz; CD_3CN): δ 9.4215 (d, J = 9.5 Hz, 1H), δ 8.384 (s, 1H), δ 8.216-8.149 (m, 2H), δ 8.084 (d, J = 10.5 Hz, 1H), δ 7.987 (d, J = 8 Hz, 1H), δ 7.645-7.615 (m, 1H), δ 7.463 (d, J = 12 Hz, 1H), δ 7.392-7.366 (m, 2H), δ 7.118 (d, J = 9 Hz, 1H), δ 6.816 (t, J = 12 Hz, 1H), δ 6.599 (t, J = 12 Hz, 1H), δ 6.089 (d, J = 12.5 Hz, 1H), δ 5.487 (q, J = 12 Hz, 1H), δ 4.424-4.324 (m, 2H), δ 3.562 (t, J = 11 Hz, 1H), δ 3.562 (t, J = 11 Hz, 1H), δ 3.452-3.382 (m,

J = 11 Hz, 2H), δ 3.055-2.910 (m, 2H), δ 2.742 (s, 3H), δ 2.401 (s, 3H), δ 1.122 (t, J = 11.5 Hz, 2H).

Synthesis of [Ir(biph)(dmbpy)$_2$](OTf)(2). [Ir(cod)(biph)(dmbpy)](OTf) (408mg, 0.5mmol) and 4,4'-dimethyl-2,2'-dipyridyl(dmbpy) (101.4mg, 0.55mmol) were placed in a 100 mL of round-bottom flask. A 20 mL of 2-ethoxyethanol was added, which was then refluxed for 10 h under N_2. After cooling the solution down to room temperature, a 300 mL of diethylether was added with vigorous stirring. The orange precipitates were formed, which were collected by filtration and washing with n-pentane and diethylether. The crude product was purified by chromatographic grade activated alumina. The yield is 82 %. ^{1}H NMR(500 MHz; CD_3CN): δ 8.463 (s, 2H), δ 8.381 (s, 2H), δ 8.079 (d, J = 6 Hz, 2H), δ 7.772 (d, J = 5 Hz, 2H), δ 7.593 (d, J = 7.5 Hz, 2H), δ 7.461 (d, J = 5 Hz, 2H), δ 7.220 (d, J = 6 Hz, 2H), δ 6.977 (t, J = 7 Hz, 2H), δ 6.730 (t, J = 7.5 Hz, 2H), δ 6.230 (d, J = 7 Hz, 2H), δ 2.660 (s, 6H), δ 2.586 (s, 6H). ^{13}C NMR (125 MHz, CD_3CN): δ 158.578, 156.473, 155.473, 153.133, 152.961, 152.174, 148.992, 133.133, 130.346, 130.071, 127.717, 126.761, 126.336, 124.912, 122.012, 22.103, 21.865. E.A: Found: C, 51.0813; H, 3.6462; N, 6.8301%. Calc. for $IrC_{37}H_{32}N_4O_3F_3S$: C, 51.56; H, 3.74; N, 6.50%. HRMS: m/z found 713.2255, calc. for 713.23.

Table S1. Crystallographic Data for [Ir(biph)(dmbpy)$_2$](OTf) (**2**).

Empirical formula	$C_{37}H_{32}F_3IrN_4O_3S$
Formula weight	861.93
Temperature	293(2) K
crystal system	monoclinic
space group	C2/c
color of crystal/description	orange/block
a	34.693(2) Å
b	11.2292(6) Å
c	18.9912(11) Å
β	107.1220(10)°
V	7070.6(7) Å^3
Z	8
Density (calculated)	1.619 Mg/m^3
Absorption coefficient	3.893 mm^{-1}
F(000)	3408
Reflections collected / unique	16134 / 5917 [R(int) = 0.0290]
Theta range for data collection	1.91 to 25.00
Data / restraints / parameters	5917 / 14 / 406
Goodness-of-fit on F^2	1.032
Final R indices [I>2sigma(I)]	$R_1 = 0.0401$, $wR_2 = 0.1230$
R indices (all data)	$R_1 = 0.0539$, $wR_2 = 0.1293$
Largest diff. peak and hole	1.118 and -1.175 e.Å^{-3}

Table S2. Selected Bond Lengths (Å) and Angles (deg) for [Ir(biph)(dmbpy)$_2$](OTf) (**2**).

Ir(1)-C(31)	2.048(7)
Ir(1)-C(312)	2.040(8)
Ir(1)-N(11)	2.018(5)
Ir(1)-N(12)	2.116(6)
Ir(1)-N(21)	2.115(6)
Ir(1)-N(22)	2.035(5)
N(11)-Ir(1)-N(22)	174.0(2)
N(11)-Ir(1)-C(312)	95.8(3)
N(22)-Ir(1)-C(312)	88.9(3)
N(11)-Ir(1)-C(31)	88.3(2)
N(22)-Ir(1)-C(31)	96.0(2)
C(312)-Ir(1)-C(31)	82.1(3)
N(11)-Ir(1)-N(21)	97.1(2)
N(22)-Ir(1)-N(21)	78.6(2)
C(312)-Ir(1)-N(21)	95.9(3)
C(31)-Ir(1)-N(21)	174.4(2)
N(11)-Ir(1)-N(12)	77.9(2)
N(22)-Ir(1)-N(12)	97.8(2)
C(312)-Ir(1)-N(12)	171.7(3)
C(31)-Ir(1)-N(12)	92.3(3)
N(21)-Ir(1)-N(12)	90.2(2)

Table S3. Calculated HOMO and LUMO energy values, and spectral data of [Ir(biph)(bpy)$_2$](OTf) and [Ir(biph)(dmbpy)$_2$](OTf).

Compound	[Ir(biph)(bpy)$_2$](OTf) (**1**)	[Ir(biph)(dmbpy)$_2$](OTf) (**2**)
Calc. HOMO (eV)	−7.287 eV	−7.084 eV
Calc. LUMO (eV)	−5.013 eV	−4.744 eV
Calc. ^{1}MLCT(nm)	392	391
^{1}MLCT (nm)	368	368
^{3}MLCT (nm)	408, 458, 514	405, 455, 512
PL λ_{max}(nm)	599	591
Φ_{PL}	0.007	0.013

Figure S1. Contour plots of the HOMO and LUMO of $[Ir(biph)(bpy)_2]^+$.

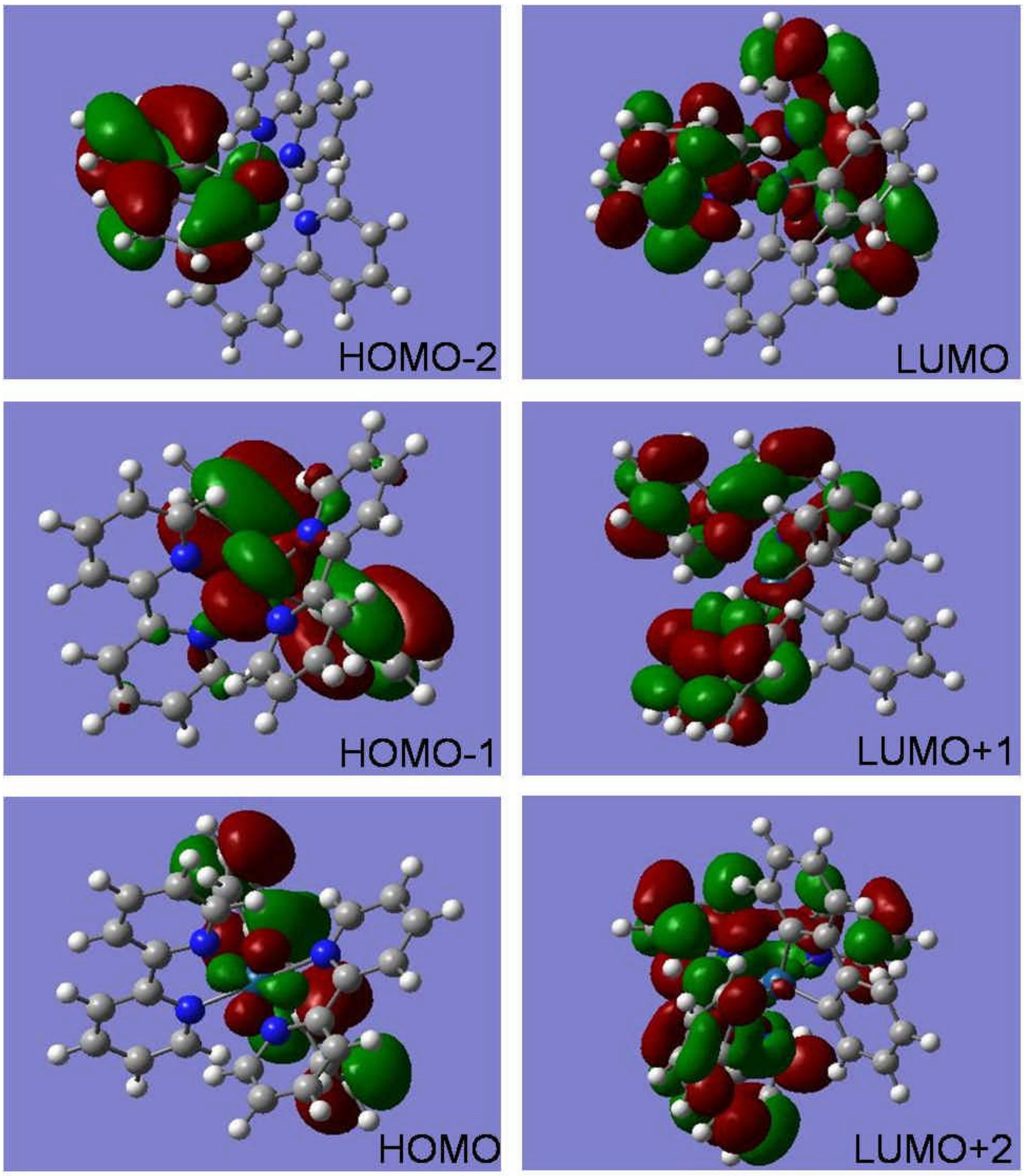

Table S4. The energy value of HOMO and LUMO of $[Ir(biph)(bpy)_2](OTf)$.

Gap	2.274
LUMO+2	−4.167
LUMO+1	−4.967
LUMO+0	−5.013
HOMO-0	−7.287
HOMO-1	−8.044
HOMO-2	− 8.089

Figure S2. Contour plots of the HOMO and LUMO of [Ir(biph)(dmbpy)$_2$]$^+$.

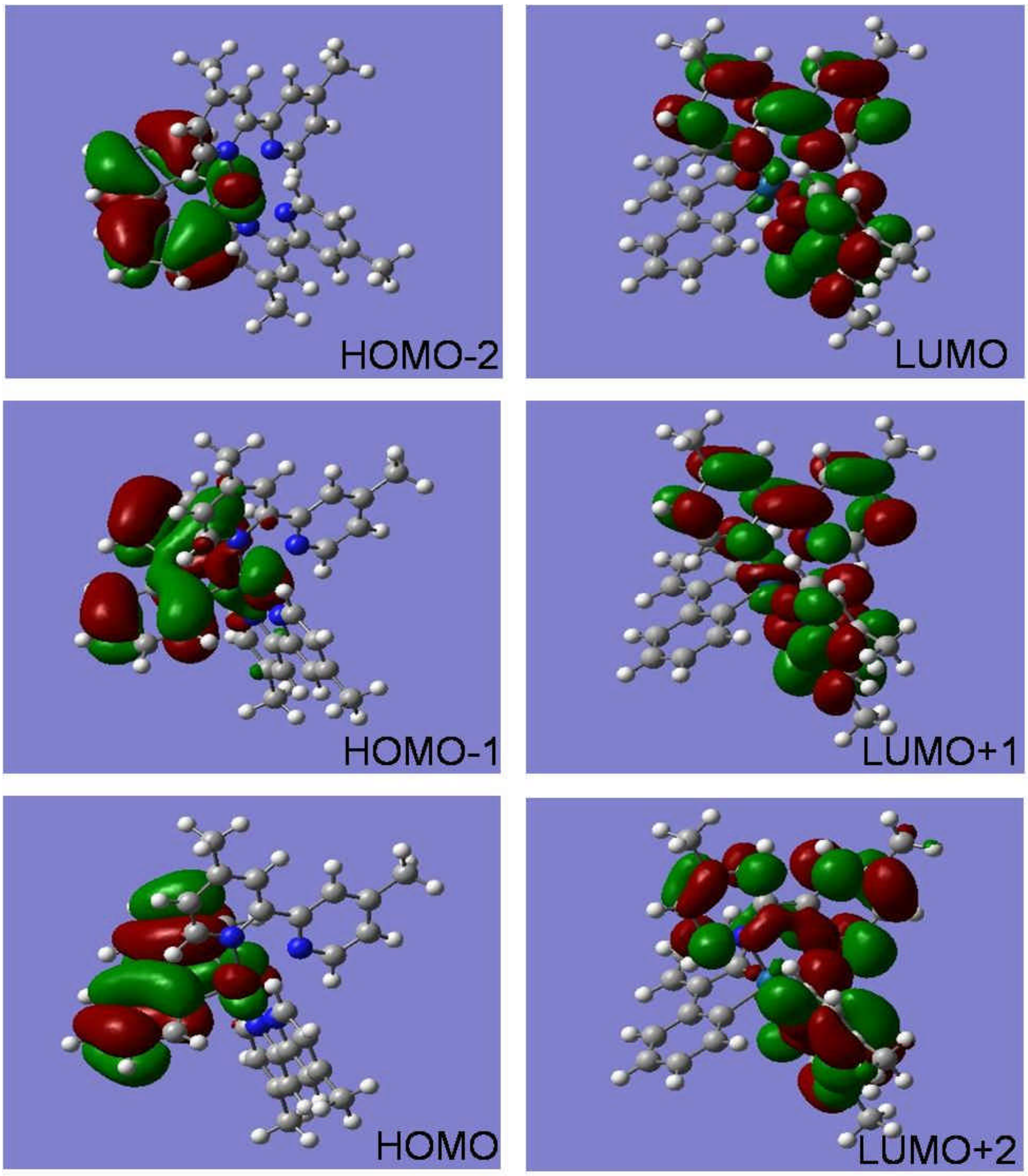

Table S5. The energy value of HOMO and LUMO of [Ir(biph)(dmbpy)$_2$](OTf).

Gap	2.340
LUMO+2	−3.830
LUMO+1	−4.697
LUMO+0	−4.744
HOMO-0	−7.084
HOMO-1	−7.819
HOMO-2	−7.887

Reference

1. P. J. Hay, W. R. Wadt , (). *J. Chem. Phys.*, **1985**, *82*, 270.

2. W. J. Hehre, R. Ditchfield, J. A. Pople, *J. Chem. Phys.*, **1972**, *56*, 2257.

3. Z. Lu, C. –H. Jun, S. R. de Gala, M. P. Sigalas, O. Eisenstein, R. H. Cratree, *Organometallics,* **1995**, *14*, 1168.